

APPLICATION OF MULTI-ENERGY COMPOSITE ENERGY STORAGE SYSTEM TECHNOLOGY IN ELECTRIC VEHICLES

Ning Li,* Fengshou Hu,* and Wenkui Ma*

Abstract

With the global environmental degradation and the reduction of non-renewable energy sources, the development of gasoline vehicles has been hindered, and new energy vehicles, mainly energy storage systems (ESs), are showing rapid development. However, the traditional pure battery ES is not enough to meet the demand for electric vehicles. In this study, the multi-energy composite ES technology with the combination of lithium-ion battery and supercapacitor is proposed for the problems of short life and low power of traditional batteries. The first is the matching and optimisation of composite ES parameters, and dynamic planning method is proposed to get the optimal lithium-ion battery and supercapacitor parameters for the target vehicle model. Secondly, the energy management strategy (EMS) of the composite ES is studied, and the EMS with working condition prediction is proposed, and the EMS of fixed rule and fuzzy rule and the retrograde comparison analysis. The experimental results show that the lithium-ion battery life is improved by 16.21%, 17.54%, and 21.11% under the new standard European driving cycle working conditions, and 29.22%, 31.74%, and 33.75% under the urban road cycle working conditions. It can be seen that the multi-energy composite energy storage technology makes the performance of the ES of electric vehicles more balanced, and the power, life and efficiency of the system are improved.

Key Words

Multi-energy composite energy storage system, parameter optimisation, energy management, supercapacitor, lithium-ion battery

1. Introduction

With the increase of global warming problem and the decrease of non-renewable energy sources, the development of traditional gasoline vehicles is hindered [1]. Electric vehicles, on the other hand, have become a new direction for the development of the automotive industry in various

* Henan Mechanical and Electrical Vocational College, Zhengzhou 451191, China; e-mail: mawenkui1986@sina.com
Corresponding author: Wenkui Ma

countries with the ability to improve the energy structure dominated by fossil energy sources and to achieve low carbonisation [2]. Most of the electric vehicles use energy storage system (ES) as the key technology to store energy for power batteries [3]. Power batteries has gone through three stages: lead-acid, nickel-hydrogen, and lithium. Lithium-ion batteries have been more used in the electric vehicle industry for their long life cycle [4]. However, lithium-ion batteries have more sensitive characteristics and require multiple replacements of their power cells during the life cycle, leading to high costs, thus limiting vehicles development [5]. In this study, a composite ES with the combination of lithium-ion battery and supercapacitor is proposed to address the problems of electric vehicle ES. To get a more balanced performance of the electric vehicle ES and thus promote electric vehicles development. The study is divided into five parts. The first part is the introduction, which describes the development of electric vehicles with energy storage as the power battery in the contemporary context of deteriorating environment and rapidly decreasing non-renewable energy sources. The second part is a literature review of the research on lithium-ion batteries and supercapacitors in various fields and the application of composite ESs in electric vehicles, and the current status of research on this aspect by many scholars. The third part is to analyse and optimise the ES parameters and to make a reasonable design of ES structure. The first subsection is to match and optimise the parameters of this system, and the second subsection is to study the energy management strategy (EMS) of this system. In the fourth section, the system is tested under the new European driving cycle (NDEC) and urban dynamometer driving schedule (UDDS) conditions, and proposed EMS using condition prediction is compared with the fixed rule and fuzzy rule energy management strategies. The fifth part is a summary and outlook of the research methodology and results.

2. Related Works

The composite ES composed of lithium-ion battery and supercapacitor, which is an auxiliary energy source with many good characteristics, has been studied and explored by many scholars. Yang *et al.* developed a method for

direct symmetric arrays growth. Experimental results showed that its capacity was similar to 160 mAh g(-1) at 5°C. The FeSiAl flake catalyst presented a novel approach for achieving efficient and rapid growth of arrays on a significant scale. This breakthrough held promising applications in various areas [6]. Liu *et al.* conducted a study on carbon and nitrogen doped Mo₂P layered materials, aiming to investigate their potential as transition metal phosphides for lithium-ion battery anode materials. Through experimental analysis, Li diffusion rate at room temperature in these materials was 10 times faster compared to that of MoS₂ and graphene. Additionally, both monolayers exhibited relatively low average open-circuit voltages, indicating that simple doping serves as an effective strategy for enhancing the performance of rechargeable battery anode materials [7]. Du *et al.* developed an equaliser to achieve high-speed arbitrary cell-to-arbitrary cell equalisation. It was compared with a conventional equaliser using a complex monitoring strategy and automatically exchanged power directly between all cell cells. Experimental results demonstrated its feasibility [8]. Yang *et al.* presented an elaborate process for preparing biochar. Experimental results showed that the device has a long cycle life and good stability up at a high power density of 9 kW centre point kg(-1) and provides an effective method for biomass recovery by pre-treating ethanol and KOH to produce carbon with HP for high energy storage applications [9].

For the structural design of the composite ES, in the face of the control voltage range, more conversion devices need to be taken, which increases the complexity and cost of this system, therefore, many scholars have studied it to achieve the optimal matching. Zhou *et al.* established a matching model of the optimal output power of the PV array with the optimised power, and analysed the performance characteristics of the PV cold storage system. The results showed that the photovoltaic system achieved a photoelectric conversion efficiency of 15.33% [10]. Sulaiman *et al.* investigated SrTiO₃ catalytic effect on hydrogen absorption properties. The results showed that SrTiO₃ exhibited good catalytic ability by lowering the onset decomposition temperature and improving its rehydrogenation kinetic properties [11].

In summary, the composite ES has been evaluated for battery life decay and has been effective in increasing its service life. However, the supercapacitor has certain limitations on materials and the low energy density of the capacitor, which can only operate in frequent charging occasions. Therefore, a multi-energy composite ES combining lithium-ion batteries and supercapacitors can better improve energy utilisation to achieve longer battery life and better performance of electric vehicles.

3. Research on the Application of Multi-Energy Composite Energy Storage System Technology in Electric Vehicles

The implementation of composite ES technology in electric vehicles is realised from two aspects. The first is the cost, conversion efficiency, and complexity to minimise

the converter power and cost. The second is to control the power of supercapacitors and batteries to raise the energy utilisation. However, when facing voltage range control, it is inevitable to take more conversion devices, which leads to increase the complexity and cost of the system [12]. Therefore, this study addresses the contradiction between the two and analyses and optimises the parameters of the ES, and based on this, the structure of the ES is reasonably designed to enhance the performance of electric vehicles.

3.1 Multi-Energy Composite ES Structure and Parameter Optimisation Analysis

Energy storage lithium-ion batteries and supercapacitors have large differences in their characteristics and cannot be directly connected together; they need to be voltage matched using a converter bidirectional DC/DC [13]. There are many different forms of power coupling for lithium-ion battery and supercapacitor combinations, so the structural forms of composite ESs can vary, including battery active structure, supercapacitor active structure, and parallel active structure. Among them, the parallel active control system topology is the one with the best performance among the three structures, and its structure is shown in Fig. 1.

The structure is equipped with bi-directional DC/DC for each energy storage source to enable individual control of each energy storage source. This structure can not only control the current of the battery at the ideal value but also solve the problem of voltage variation at both ends of the capacitor. Therefore, the evaluation function of composite ES is established to evaluate the cost of this system during its life cycle, and the comprehensive usage cost is used as the objective function to match and optimise it to obtain better performance of composite ES. The cost definition equation of composite ES is shown in (1).

$$C_0 = C_b + C_{uc} + C_D + C_c \quad (1)$$

In (1), C_c is the cost of electricity, C_D is the cost of DC/DC, C_{uc} is the cost of the supercapacitor pack, C_b is the cost of the lithium-ion battery pack for the composite ES, and C_0 is the total cost of fee and ES. This definition is calculated by converting the cost of composite ES to each kilometre, then the cost per kilometre of the system $Cost_{bL}$ is defined as shown in (2).

$$Cost_{bL} = \frac{C_b + C_{uc} + C_D + C_c}{S_N} \quad (2)$$

In (2), S_N is the total mileage of the car when the lithium-ion battery life is exhausted, and its calculation formula is shown in (3).

$$S_N = \frac{20S}{B_{1s} \sum_{k=1}^{k_N} \left(e^{B_{2s}(n-1)} \frac{P_b(k)}{V_b(k)} \Delta t \right)} \quad (3)$$

In (3), S_1 is the mileage of a single driving condition, Δt is the time interval, k_N is the total number of sampling points for a single condition, and $V_b(k)$ is the battery voltage at the k moment. And the cost of DC/DC is

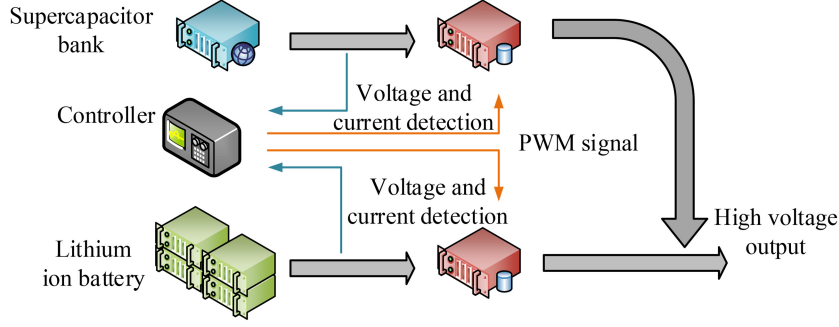


Figure 1. Parallel active control system topology.

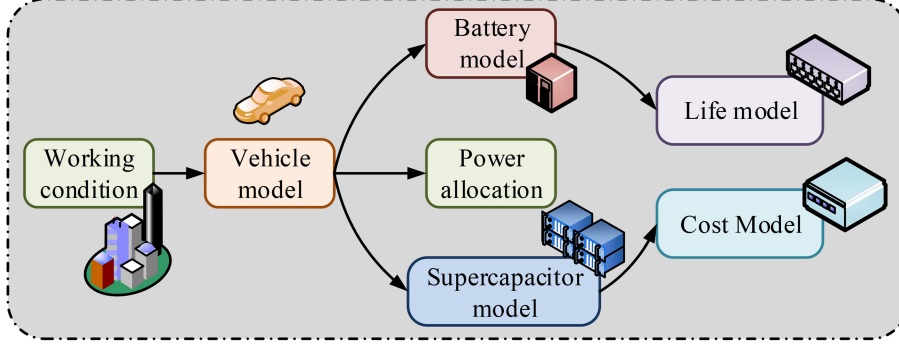


Figure 2. Information flow between components of a composite ES.

calculated as shown in (4) after the power distribution of the supercapacitor at each time point.

$$C_D = C_{d0} \max [P_c(k)] \quad (4)$$

In (4), C_{d0} is the cost of DC/DC per unit of power. The lithium-ion battery pack belongs to the main energy source in the system, and it has to meet the requirements for power while meeting the requirements for driving range. The formula for calculating the cost of lithium-ion battery pack is shown in (5).

$$C_b = \max \left[\frac{C_{be} S_x}{S_1} \sum_{k=1}^{k_N} (P_r(k) + P_{loss}(k) - P_c(k)) \Delta t, C_{bp} \max(P_b(k)) \right] \quad (5)$$

In (5), S_x is the driving range, C_{bp} is the price per kW of battery, and C_{be} is the price per kWh of capacitor. Different parameters have different effects on the system performance of lithium-ion batteries and supercapacitors, and the power demand of the car driving under both NEDC and UDDC conditions obeys a normal distribution [14]. For the optimal energy management of the two operating conditions under car driving, the dynamic planning method can be used to solve the problem. And the information flow between the components during the operation of the car is shown in Fig. 2.

The NEDC and UDDC conditions are used to determine the speed and acceleration of the vehicle to obtain the power requirements of the vehicle. The

parameters of lithium-ion battery and supercapacitor are determined for NEDC and UDDC operating conditions of the electric vehicle to determine the power demand at each moment $P_c(k)$. The relationship between the capacitor power distribution factor $u(k)$ and $P_c(k)$ at the time the vehicle is running $k\Delta t$ is shown in (6).

$$P_c(k) = u(k)P_r(k) \quad (6)$$

After the sub-allocation of battery and supercapacitor by (6), the battery voltage $v_b(k)$, supercapacitor voltage $v_c(k)$, battery current $i_b(k)$, supercapacitor current $i_c(k)$, and supercapacitor energy state $SOE_c(k)$ can be obtained at each moment, and then the cost of the system $Cost_{bL}$ is obtained according to the battery model and the cost model of composite ES. For the finding of the optimal supercapacitor power allocation factor $u(k)$, a dynamic planning algorithm can be used, and the dynamic planning under this system is shown in Fig. 3.

The dynamic programming method can perform a global optimal solution for optimal energy management because of its advantage of backward seeking. Taking $SOE_c(k)$ as the system state variable and the time interval Δt as the step size, the number of working intervals is calculated as shown in (7).

$$k_N = \frac{T_c}{\Delta t} \quad (7)$$

In (7), T_c represents the total time length of the working condition. And the state transfer function of the

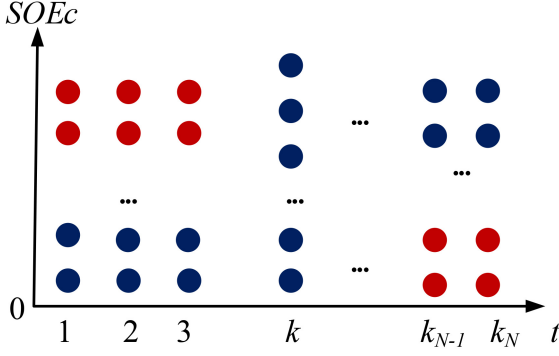


Figure 3. Dynamic programming diagram of composite ES.

supercapacitor energy state is defined as shown in (8).

$$x_{k+1} = -\frac{u_k P_r(k) + P_{\text{loss-sc}}(k)}{0.5 C_{\text{sc}0} v_{\text{sc}0}^2} \Delta t + x_k \quad (8)$$

In (8), $u_k = u(k)$ represents the value of the control quantity at $k\Delta t$, $x_{k+1} = x(k+1)$ is the state variable value at the moment, $(k+1)\Delta t P_{\text{loss-sc}}(k)$ represents the power loss of the supercapacitor at the moment $k\Delta t$, $C_{\text{sc}0}$ represents the initial capacity, and $v_{\text{sc}0}$ represents the initial voltage. Based on the analytical process of the evaluation of the composite ES by (7) and (8), the performance expression of the system cost is shown in (9).

$$J = g_{k_N}(x_{k_N}) + \sum_{k=1}^{k_N} \left[B_{1s}(e^{B_{2s}(n-1)} \frac{(1-u_k)P_r(k)}{V_b(k)} \Delta t) + P_{\text{loss}}(u_k) \Delta t \right] \quad (9)$$

In (9), $B_{1s}(e^{B_{2s}(n-1)} \frac{(1-u_k)P_r(k)}{V_b(k)} \Delta t)$ represents the effect of different power allocation factors on the system lifetime, and $P_{\text{loss}}(u_k) \Delta t$ represents different power allocation factors effect on the system power consumption cost. For the management of composite ES, the dynamic programming method is the most appropriate solution for the optimal energy management when the vehicle is facing NEDC operation and UDDC operation.

3.2 Research on EMS of Multi-Energy Composite ES

To better control the battery and supercapacitor effectively, a reasonable power distribution strategy is designed to ensure that the system can operate efficiently [15]. To make the supercapacitor have enough energy to provide acceleration power when the car is accelerating and at the same time there is enough space for energy recovery. There are two main steps to study the EMS, first is to establish the composite ES to provide the basic conditions for the EMS development. The second is to set up a reasonable EMS so that the strategy can take advantage of each energy storage source [16], [17]. Three energy management strategies are made for the future driving conditions of the vehicle, a strategy based on fuzzy control rules, a strategy based on fixed rules, and a strategy based on working

condition prediction. Among them, the fuzzy control rule-based strategy utilises fuzzy logic and fuzzy reasoning, and its structure is shown in Fig. 4.

Fuzzy logic is a nonlinear control method that can be used to deal with imprecise information [18], [19]. Among them, the fuzzy inference system is composed of four parts: knowledge base, fuzzy inference, fuzzification interface and defuzzification. For different modes of operation of electric vehicles, system efficiency in the present mode is shown in (10).

$$\eta_{\text{sys}} = \frac{P_{\text{out}}}{P_{\text{in}}} \quad (10)$$

In (10), η_{sys} is the system efficiency, P_{in} is the system input power, and P_{out} is the output power. In the fuzzy layer, the input variables are fuzzified and the affiliation of the output is obtained with the expression shown in (11).

$$O_i^1 = \begin{cases} \mu_{A_i}(x), & i = 1, 2 \\ \mu_{B_{i-2}}(y), & i = 3, 4 \end{cases} \quad (11)$$

In (11), $\mu_A(x)$ is the fuzzy set affiliation function, the expression of which is shown in (12).

$$\mu_A(x) = \frac{1}{1 + \left(\frac{x-c_i}{a_i}\right)^{2b_i}} \quad (12)$$

In (12), $\{a_i, b_i, c_i\}$ is the adaptive parameter and the fuzzy controller allocates the power by the above equation. The fixed rule-based EMS for composite ESs, which is simple and fast in operation, is the most commonly used strategy for energy management strategies [20], [21]. This strategy sets three thresholds for the power of the Li-ion battery for three energy state levels: low, medium, and high. The power allocation logic based on fixed rules is shown in Fig. 5.

The strategy integrates the charge and discharge current of lithium-ion battery and energy state of the supercapacitor to reduce the large rate of battery discharge to a certain extent. And the corresponding power allocation scheme is set for the power demand and the energy state of supercapacitor during the actual operation of the vehicle. And the EMS of the composite ES based on and working condition prediction is a working condition prediction model constructed by analysing historical data [22], [23]. This strategy focuses on making online prediction of the driving working conditions of electric vehicles in the future time, and realises more effective online power allocation, and its fuzzy EMS is shown in Fig. 6.

The strategy is able to predict the unknown operating conditions of the car driving, prompting the supercapacitor to make adjustments to the energy state in advance, reserving space for energy recovery in subsequent operating conditions, as well as providing the energy needed to drive the car in subsequent operating conditions. Vehicle operating state is only related to the current operating state, and is independent of the past operating state, and this process is very much in accordance with the Markov process [24], [25]. The Markov process is a stochastic process without posteriority and has a high similarity with

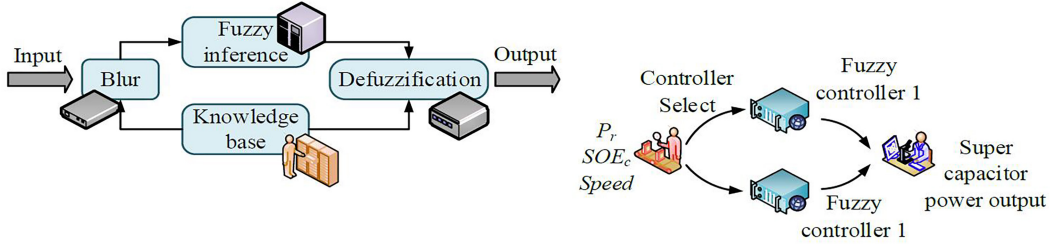


Figure 4. EMS structure of fuzzy control rules.

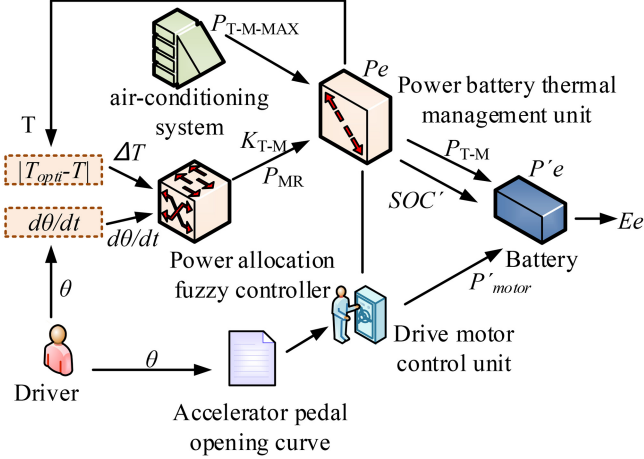


Figure 5. EMS logic by fixed rules.

the driving conditions of the car. Where the velocity is v_k and the acceleration is a_k at the moment of the car's operation at k , the equation defining the Markov chain state is shown in (13).

$$X_k = (v_k, a_k) \quad (13)$$

The defining equation for the joint distribution probability of the velocity, and acceleration of the car running at the next moment $k + 1$ is shown in (14).

$$P(v_{k+1}, a_{k+1} | v_k, a_k) = p_{k,k+1} \quad (14)$$

The state transfer matrix of Markov chain is obtained by (14), but the conditional probability of transferring the current state condition to every other state needs to be obtained, and the conditional probability of the next state of each state can be obtained by the historical working condition statistics, which is defined as shown in (15).

$$p_{ij} = P(j | i) \quad (15)$$

In (15), p_{ij} is the conditional probability of the occurrence of the state j under the condition i . The conditional probability $P(j | i)$ can be obtained from the statistics of the vehicle history data, and its calculation formula is shown in (16).

$$p_{ij} = \frac{N_{ij}}{N_i} \quad (16)$$

In (16), N_{ij} is the number of times the state i is transferred to the state j in the historical working condition

data, and N_i is the total number of times the state i is transferred to all states in the historical working condition data. The Markov chain constructs the prediction model of the operating conditions of the vehicle to predict the future conditions, and on this basis, the energy allocation of the composite ES is carried out to make the power allocation of this system more accurate.

4. Performance Testing of Multi-Energy Composite ES Technology in Electric Vehicles

To verify the actual performance of composite ES, the performance of composite ES composed of single battery, lithium-ion battery, supercapacitor and main controller components is tested under three energy management strategies, as well as the performance of the composite ES under working conditions. To ensure data reliability, this study will be conducted in the same experimental environment and using the same experimental equipment. The experimental environment is room temperature 25°C and humidity 15%–90%, and the experimental equipment uses a battery simulator model EVT 300-750-2×80 kW IGBT, CAN analyser model ZLG USBCAN-2EU, and power analyser model Ziyuan Electronics PA6000 to collect Li-ion battery, supercapacitor and DC current and voltage. The main equipment is shown in Table 1.

To test working performance of the composite ES, working operation under pure battery pack will be used to compare and analyse with the composite ES that introduces supercapacitor as an auxiliary energy source. Before the test, the SOC needs to be adjusted by discharging the battery pack at 1C constant current to a minimum voltage of 3.0 V for a single cell, and then leave it for 30 min. Then, charge it with 1C constant current to the highest voltage of 4.2 V, discharge it to the position of SOC of 80%, and use it as the base working condition for testing. The battery voltage and current results obtained from the test are shown in Fig. 7.

As can be seen from Fig. 7, both the NEDC condition and UDSS condition consume less power gradually as the test time increases. In the NEDC condition, the power consumption is 5.1 Ah; the energy generated is 1,736.73 Wh; the accumulated power consumption is 7.4 Ah; the accumulated energy consumption is 2,572.8 Wh; and the total duration of this condition is 1,190 s. The three designed energy management strategies were introduced into the main controller of composite ES, and its performance was tested under different driving conditions. Firstly, the energy strategy with fixed rules was tested.

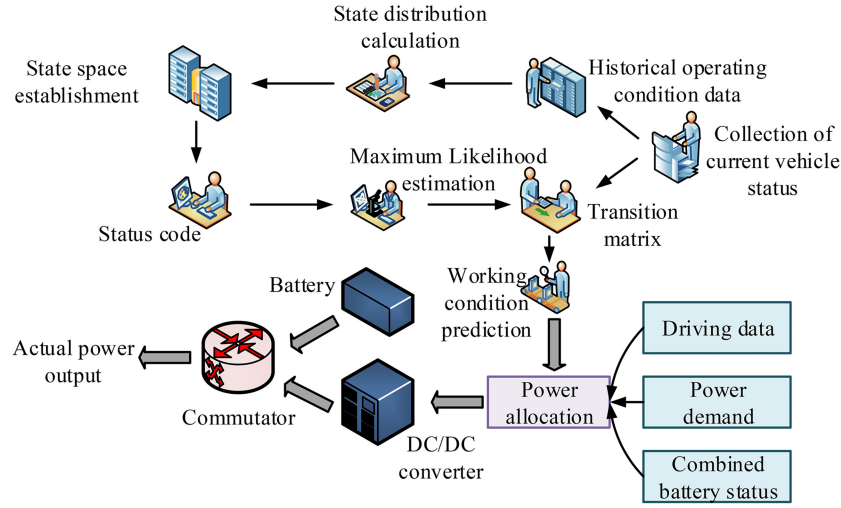


Figure 6. Schematic diagram of power distribution and control for composite ES.

Table 1
Main Experimental Equipment

Serial number	Name	Model	Parameter
1	Low voltage power supply	HS-250T-12	12 V/20 A
2	CAN analyser	ZLG USBCAN-2EU	3thoroughfare
3	Power Analyser	ZLG PA6000	4thoroughfare
4	Cell simulator	EVT 300-750-2×80 kW IGBT	800 V/300 A 0.1%FS
5	Upper computer	/	/
6	High/low voltage wiring harness	/	/

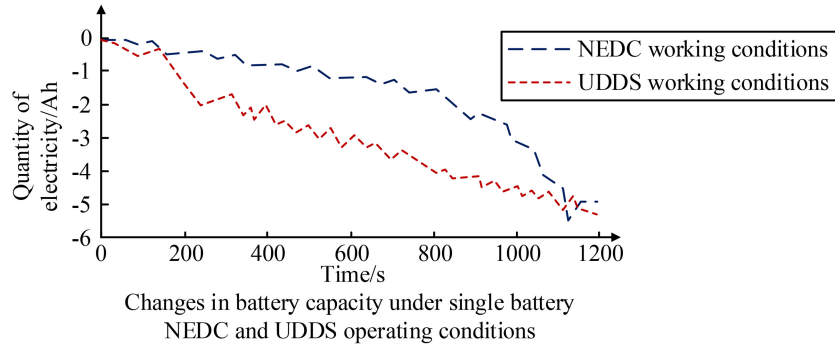


Figure 7. Electric quantity change curve of pure battery pack under NEDC and UDSS conditions.

From Fig. 8, it can be seen that the current and voltage performance of the composite ES under UDSS and NEDC operating conditions. In the UDSS operating conditions, the utilisation rate of system current and voltage increases with the passage of testing time. In Fig. 8(a), during the testing period 800 s ago, the system maintained stable performance. However, during the time period of 800 to 1,000 s, the phenomenon of energy storage depletion of supercapacitors was observed, during which the current and voltage reached 127 A and 226 V, respectively, while the voltage of the relevant

supercapacitors was recorded as 193 V. In Fig. 8(b), the supercapacitor provides significant auxiliary power to the system. At this point, the capacitor effectively supports the utilisation of system voltage and current, with the recorded current range maintained at 0.98 A and the voltage maintained at 112 V, while the capacitor voltage reached the dominant performance of 227 V. Revealed the benefits of supercapacitors in providing auxiliary power under dynamic conditions, as well as their importance in maintaining stable system operation. Before the test, the SOE of the Li-ion battery pack is adjusted to 80% as the

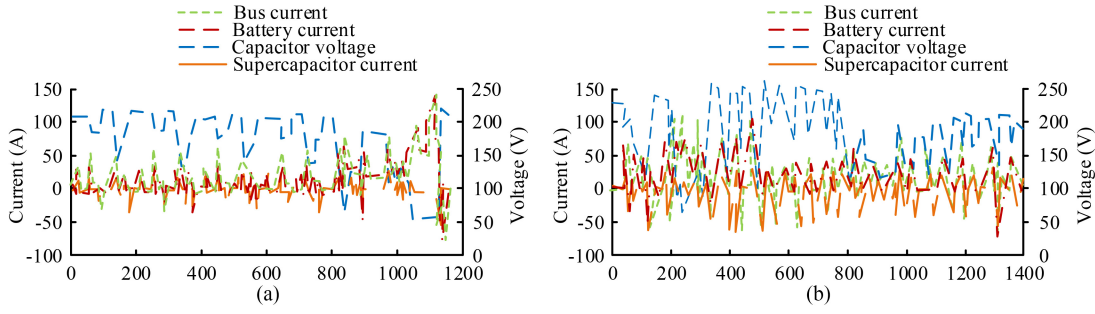


Figure 8. Test waveforms of NEDC and UDDS operating conditions based on fixed rule strategy: (a) NEDC working condition test waveform and (b) UDDS working condition test waveform.

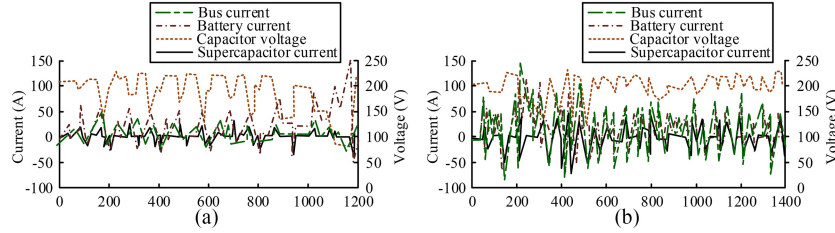


Figure 9. Test waveforms of NEDC and UDDS operating conditions based on fuzzy EMS: (a) NEDC working condition test waveform and (b) UDDS working condition test waveform.

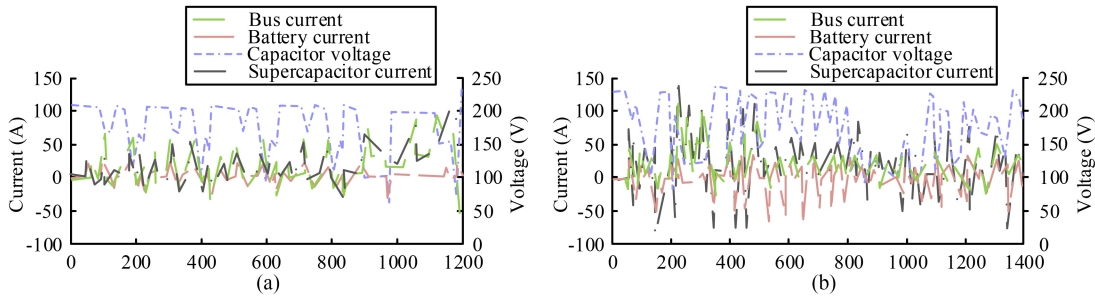


Figure 10. Test waveforms of NEDC and UDDS operating conditions based on EMS for condition prediction: (a) NEDC working condition test waveform and (b) UDDS working condition test waveform.

initial point of the test, and the waveform diagram of each signal is obtained, and the results are shown in Fig. 9.

As shown in Fig. 9, under the UDDS operating condition, the current and voltage significantly increase with time, indicating the effective utilisation of energy. In Fig. 9(a), under NEDC conditions, the system exhibits steady-state behaviour before 916 s of testing, with a current maintained at 29 A, and a voltage maintained at 108 V. At the same time, the capacitor exhibits a voltage performance of 203 V. In Fig. 9(b), during the later high-speed stage of the testing cycle, the supercapacitor provides significant auxiliary power. Throughout the testing period, the current and voltage remained stable at 1.24 A and 137 V, while the capacitor maintained a voltage performance of 228 V. In addition, the EMS controller of the composite ES receives inputs, including the energy state of the supercapacitor, changes in vehicle speed, and power demand to predict and regulate system operating conditions. Before the test, the SOE of the Li-ion battery pack was adjusted to 80% as the initial point of the test,

and the waveform graphs of each signal were obtained, and the results are shown in Fig. 10.

As shown in Fig. 10, the utilisation rate of supercapacitors gradually reaches its maximum over time in the UDDS and NEDC operating conditions. Under NEDC operating conditions, in Fig. 10(a), the overall current and voltage show a stable state throughout the entire testing cycle. Especially during the time period of 829 s to 1,200 s, the current and voltage remained stable at 79 A and 163 V, respectively. At this time, the voltage performance of the capacitor was 198 V. In Fig. 10(b), as the testing time progresses to the high-speed stage, the current and voltage remain at 1.74 A and 136 V, and the voltage performance of the capacitor is 221 V. Verified the performance indicators of the supercapacitor throughout the entire testing period. The battery life analysis of the composite ES under UDDS operating conditions and NEDC operating conditions, the results of which are shown in Table 2.

As can be seen from Table 2, in the NEDC condition, the power supply of a single battery, calculated by the

Table 2
The Influence of Composite ES on Battery Life Under NEDC and UDDC Conditions

Working condition type	/	Single battery	Fuzzy rules	Fixed rules	Working condition prediction
NEDC working conditions	Measured mileage	73,762	85,351	86,398	88,837
	Predicted mileage	72,857	85,269	85,733	87,974
	Equivalent electric quantity	8.01	6.68	6.61	6.87
	Equivalent power reduction percentage	/	13.71	14.75	17.11
	Error between measured and predicted values	1.31	0.14	0.81	1.03
UDDC operating conditions	Measured mileage	78,997	101,742	103,601	105,233
	Predicted mileage	78,136	97,327	100,319	100,442
	Equivalent electric quantity	9.83	7.86	7.11	6.95
	Equivalent power reduction percentage	/	22.67	24.18	25.22
	Error between measured and predicted values	1.19	4.52	3.31	4.69
	Increased longevity	0.02	28.93	31.46	33.48

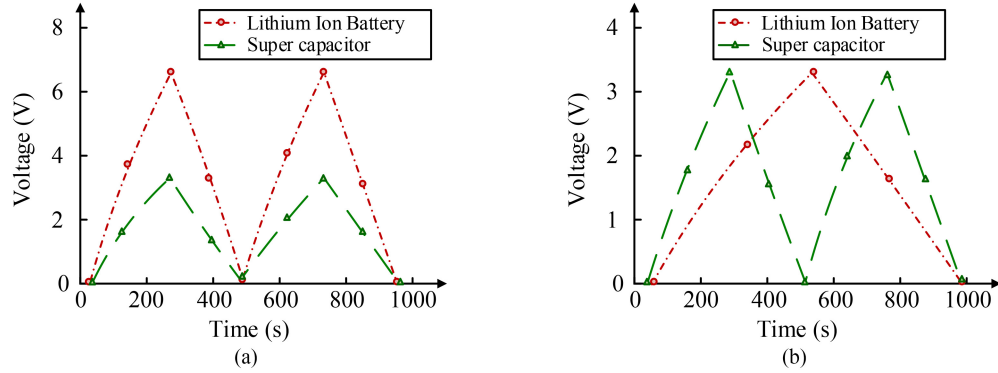


Figure 11. Testing battery and supercapacitor performance under extreme weather conditions: (a) performance results of batteries and supercapacitors under extreme high temperature conditions and (b) performance results of batteries and supercapacitors under extreme low temperature conditions.

lithium-ion battery service life model, its equivalent power is 8.01 Ah, and the mileage of a single NEDC condition is 10.78 km, when the lithium-ion battery pack capacity decreases by 25%, the car travels 85,351 km, 86,398 km, and 8,837 km in the NEDC condition under the three strategies, respectively. In under UDDC conditions, the power supply of a single battery, calculated by the lithium-ion battery life model, has an equivalent power of 9.83 Ah, and the mileage of a single NEDC condition is 12.23 km. When the capacity of the lithium-ion battery pack decreases by 25%, the car travels 101,742 km, 103,601 km, and 105,233 km in NEDC conditions under the three strategies, respectively. It can be seen that, the composite ES has better advantages for extending the service life of Li-ion batteries compared to pure battery packs. To verify the actual performance of the

composite ES, the battery and supercapacitor performance were tested under extreme weather conditions, and the results are shown in Fig. 11.

The voltage response of the composite ES under extreme weather conditions is shown in Fig. 11. In Fig. 11(a), the voltage fluctuation of the system in a high-temperature environment, with the battery voltage fluctuating in the range of 0.11 V to 6.83 V, shows a significant time dependence. At the time nodes of 23 s, 446 s, and 974 s, the measured voltage values were 0.12 V, 0.10 V, and 0.11 V, respectively, indicating moderate fluctuations. At 238 s and 782 s, the voltage values reached higher values of 6.79 V and 6.83 V, respectively. Supercapacitors exhibit voltage peaks of 3.67 V and 3.59 V. In Fig. 11(b), the voltage range of the system is reduced

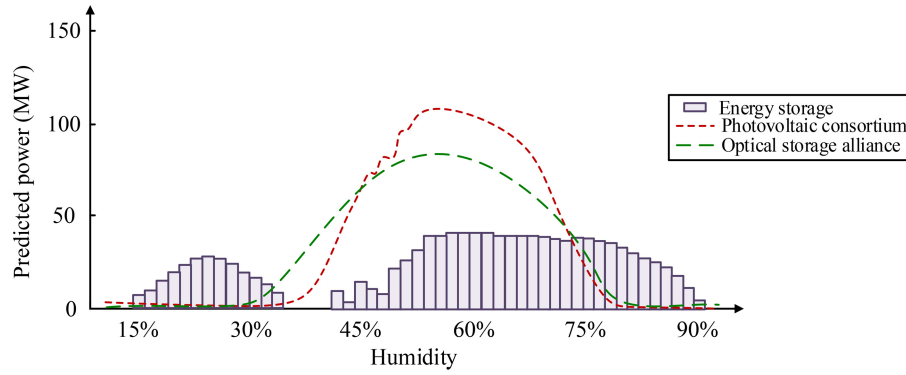


Figure 12. The impact of different humidity levels on system performance.

to 1.09 V to 3.37 V under low temperature conditions. The voltage values at time nodes of 25 s, 559 s, and 991 s are 0.08 V, 0.11 V, and 0.11 V. At 229 s and 793 s, the voltage values are 3.31 V and 3.24 V. The supercapacitor reaches a maximum voltage of 3.33 V in this environment. Revealing the voltage characteristics of system components at temperature extremes is crucial for evaluating the temperature adaptability of composite ESs. The evaluation results of the impact of different humidity on system performance are shown in Fig. 12.

As shown in Fig. 12, the power prediction analysis of the combined photovoltaic power generation and ES under different humidity levels. Before the relative humidity reaches 30%, the predicted power of the photovoltaic combined system and the photovoltaic combined system is at an extremely low level, only reaching 0.15 MW, showing a preliminary trend of the impact of relative humidity on system performance. When the humidity is within the range of 30% to 81%, the power of these two combined schemes is significantly improved, with predicted power of 68 MW and 123 MW, respectively. Compared to the photovoltaic joint scheme, the composite ES exhibits high stability in the humidity range of 15% to 30%, operating at an average predicted power of 29 MW. In the humidity range of 42% to 90%, the average predicted power of the composite ES further increases to 45 MW. It can be seen that under changing humidity conditions, the power output of the composite ES not only maintains a certain level but also increases with increasing humidity, reflecting the potential of the ES in adapting to environmental variations.

5. Conclusion

With the aggravation of global warming problem and the drastic reduction of non-renewable energy, the development of traditional gasoline vehicles has been restricted, thus promoting the development of new energy electric vehicles. However, the traditional pure battery ES cannot meet people's daily travel needs due to its power density, and battery life constraints. This study proposes a composite ES with the combination of lithium-ion battery and supercapacitor to address the problems of traditional electric vehicle ES. The experimental results show that the supercapacitor is utilised to the maximum extent with the increase of running time in both UDDS and NEDC

operating conditions. And in the last high speed part, the energy of supercapacitor maximises the battery power and provides better auxiliary power, which makes the whole process of car operation close to stable acceleration. In the NEDC condition, the equivalent amount of power supplied by a single battery is 8.01 Ah, and when the lithium-ion battery pack capacity decreases by 25%, the car travels 85,351 km, 86,398 km, and 8,837 km in the NEDC condition under the three strategies. In the UDDS condition, the equivalent amount of power supplied by a single battery is 9.83 Ah, and when the lithium-ion battery pack capacity decreases by 25%, the car travels 85,351 km, 86,398 km, and 8,837 km in the NEDC condition under the three strategies. It can be seen that the energy of the supercapacitor will not be depleted during the actual operation of the car at high speed and can be recharged during the deceleration process with high utilisation rate, and the composite ES has a good effect on the battery life. However, the EMS proposed in this study is an experiment based on fixed car models and fixed working conditions, and further research and discussion are needed for the actual situation.

Funding

This study was supported by the Henan Provincial Science and Technology Research Project (222102220070) and Key Scientific Research Projects of higher education in Henan Province (22A460012).

References

- [1] X. Lv, S. Ji, V. Linkov, X. Wang, H. Wang, and R. Wang, Three-dimensional N-doped super-hydrophilic carbon electrodes with porosity tailored by Cu_2O template-assisted electrochemical oxidation to improve the performance of electrical double-layer capacitors, *Journal of Materials Chemistry A*, 9(5), 2021, 2928–2936.
- [2] V. Adimule, S. Nandi, and H.J. Adarsha, A facile synthesis of Cr doped WO_3 nanostructures, study of their current-voltage, power dissipation and impedance properties of thin films, *Journal of Nano Research*, 67(1), 2021, 33–42.
- [3] A. Paul, A. Cano, J. Benavides, and F. Jurado, Feasibility study of a renewable system (PV/HKT/GB) for hybrid tramway based on fuel cell and super capacitor, *IET Renewable Power Generation*, 15(3), 2021, 491–503.
- [4] Y. Li, B. Huang, X. Zhao, Z. Luo, S. Liang, H. Qin, and L. Chen, Zeolitic imidazolate framework-L-assisted synthesis

- of inorganic and organic anion-intercalated hetero-trimetallic layered double hydroxide sheets as advanced electrode materials for aqueous asymmetric super-capacitor battery, *Journal of Power Sources*, 527(15), 2022, 2–11.
- [5] Z. Wu, Y. Zhao, and N. Zhang, A literature survey of green and low-carbon economics using natural experiment approaches in top field journal, *Green and Low-Carbon Economy*, 1(1), 2023, 2–14.
- [6] X. Yang, L. Wu, J. Hou, B. Meng, R. Ali, Y. Liu, and X. Jian, Symmetrical growth of carbon nanotube arrays on FeSiAl micro-flake for enhancement of lithium-ion battery capacity, *Carbon: An International Journal Sponsored by the American Carbon Society*, 189(2), 2022, 93–103.
- [7] G. Li, G. Xu, Y. Ding, Z. Huang, X. Yang, and L. Ma, Evaluation on thermal performance of liquid-cooling structures for high-power lithium-ion battery pack, *International Journal of Energy Research*, 46(5), 2022, 6099–6111.
- [8] X. Liu, S. Lin, J. Gao, H. Shi, S.-G. Kim, Z. Chen, and H. Lee, Enhanced performance of Mo₂P monolayer as lithium-ion battery anode materials by carbon and nitrogen doping: a first principles study, *Physical Chemistry Chemical Physics*, 23(6), 2021, 4030–4038.
- [9] G. Du, G. Zhang, S. Yu, H. Yu, W. Lin, and W. Le, An any-unit-to-any-unit method for hybrid-structured voltage equalizer in series-connected battery/super-capacitor strings, *International Journal of Circuit Theory and Applications*, 50(6), 2022, 2016–2034.
- [10] W. Yang, C. Zhu, L. Li, W. Wang, and Z. Yang, Pitaya peel derived carbons with ultra-high specific surface area for solid-state flexible asymmetric supercapacitors, *Functional Materials Letters*, 14(5), 2021, 2–4.
- [11] X. Zhou, Y. Zhang, X. Ma, G. Li, Y. Wang, C. Hu, J. Liang, and M. Li, Performance characteristics of photovoltaic cold storage under composite control of maximum power tracking and constant voltage per frequency, *Applied Energy*, 172(6), 2022, 1120–1132.
- [12] Q. Yu, C. Zhang, Y. Lu, Q. Kong, H. Wei, Y. Yang, Q. Gao, Y. Wu, and A. Sciacovelli, Comprehensive performance of composite phase change materials based on eutectic chloride with SiO₂ nanoparticles and expanded graphite for thermal energy storage system, *Renewable Energy*, 172(3), 2021, 1120–1132.
- [13] N.N.I. Sulaiman, M.S. Yahya, N. Sazelee, N.A. Ali, N.S. Mustafa, M. Ismail, *et al.* An investigation on the addition of SrTiO₃ to the hydrogen storage properties of the 4MgH₂-Li₃AlH₆ composite, *International Journal of Energy Research*, 46(6), 2022, 8030-8041.
- [14] Q. Han, Y. Sheng, and X. Zhang, Preparation of a multifunctional P-CF@Mn₃O₄ composite as a structural anode material, *New Journal of Chemistry*, 45(35), 2021, 15808–15817.
- [15] M. Yang, Research on vehicle automatic driving target perception technology based on improved MSRPN algorithm, *Journal of Computational and Cognitive Engineering*, 1(3), 2022, 147–151.
- [16] G. Xu, Optimized lithium-indium chloride solid electrolyte for high energy all-solid-state batteries, *Nano Hybrids and Composites*, 34(3), 2022, 3–8.
- [17] X. Wang, Q. Wang, L. Shuang, and C. Chen, A Markov model for subway composite energy prediction, *International Journal of Computer Systems Science and Engineering*, 39(2), 2021, 237–250.
- [18] S. Bae, J. Oh, J. Kim, E.R. Baek, and Y. Nam, Energy performance analysis of textile and capillary tube composite panel system by computational fluid dynamics and real-scale experiments, *Energy and Buildings*, 258(5), 2022, 2–10.
- [19] X. Kong, L. Jiang, Y. Yuan, and X. Qiao, Experimental study on the performance of an active novel vertical partition thermal storage wallboard based on composite phase change material with porous silica and microencapsulation, *Energy*, 239(15), 2022, 2–17.
- [20] R.K. Al-Hamido, A new neutrosophic algebraic structures, *Journal of Computational and Cognitive Engineering*, 2(2), 2023, 150–154.
- [21] H. Yu, S. Niu, L. Jian, X. Lei, and Z. Shao, Enhancing electric vehicle penetration and grid operation performance in old residential communities through hybrid AC/DC microgrid reconstruction, *Applied Energy*, 347(1), 2023, 2–15.
- [22] J. Cui, Q. Tan, and L. Liu, Environmental benefit assessment of second-life use of electric vehicle lithium-ion batteries in multiple scenarios considering performance degradation and economic value, *Environmental Science and Technology*, 57(23), 2023, 8559–8567.
- [23] T. Simolin, K. Rauma, A. Rautiainen, and P. Jarventausta, Communicational aspects in hierarchical real-time control of electric vehicle charging: Available information and its value, *IET Generation, Transmission & Distribution*, 17(14), 2023, 3152–3167.
- [24] S. Barmada, A. Musolino, J. Zhu, and S. Yang, A novel coil architecture for interoperability and tolerance to misalignment in electric vehicle WPT, *IEEE Transactions on Magnetics*, 59(5), 2023, 2–5.
- [25] V. Arjun and M.P. Selvan, Assessing the need for network-based technical constraints in economic optimization of electric vehicle charging, *Electrical Engineering*, 105(3), 2023, 1629–1641.

Biographies



Ning Li received the M.S. degree from the School of Mechanical and Electrical Engineering, Henan Agricultural University in 2012. Her current research interest is vehicle engineering.



Fengshou Hu received the M.S. degree from the School of Mechanical and Electrical Engineering, Henan Agricultural University in 2009. His current research interest is vehicle engineering.



Wenkui Ma received the Ph.D. degree from the School of Mechanical Engineering, Tianjin University, Tianjin, China. His research interests include high precision machining and inspection of parts.